Proceedings of the 1997 IEEE
International Conference on Robotics and Automation
Albuquerque, New Mexico - April 1997

Mobile Robot Motion Estimation from a Range Scan Sequence

Javier Gonzalez* and Rafael Gutierrez**

* Departamento de Ingenieria de Sistemas y Automatica, University of Malaga
Campus Teatinos, 29080 Malaga, SPAIN. E-mail: jgonzalez@ctima.uma.es
**Departamento de Electronica. University of Jaen
Alfonso X El Sabio, 23700 Linares, SPAIN. E-mail: rgutierr@piturda.ujaen.es

Abstract

This paper presents an innovative algorithm to estimate the motion parameters of a mobile robot equipped with a radial laser rangefinder. Our method is based on the spatial and temporal linearization of the range function, which leads to a velocity constraint equation for the scanned points. Besides, the proposed formulation computes the motion vectors of the scanned points as they move from scan to scan in the sequence. This motion field can be very useful for a number of applications including detection and tracking of moving objects. Experimental results are presented, showing that good results are achieved with both real and synthetic data.

1. Introduction

We consider the problem of estimating the instantaneous motion parameters of a mobile robot equipped with a radial laser rangefinder. Basically, such a sensor consists of a pulsed infrared laser transmitter/receiver pair and a mirror that rotates about the vertical axis deflecting the laser beam so that it emerges parallel to the ground (figure 1).

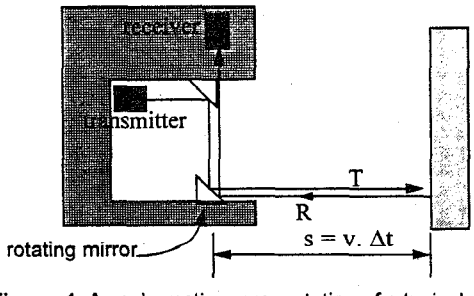

Figure 1. An schematic representation of a typical radial laser rangefinder.

By timing the amount of time it takes for a transmitter pulse to bounce off a target and be detected by the receiver, the scanner provides a two dimensional (polar) representation of the environment. The field of view uses to vary from 180 up to 360 degrees. Other characteristics, including accuracy, points per revolution, resolution, maximum and minimum range, scanning speed, etc. depend on the kind of sensor.

The formulation we present here is based on computing the motion field that arises in a range scan when the sensor moves relative to the environment. A vector in this field indicates the motion of each range point between consecutive scans.

In our study we assume that the environment is rigid, that is, it is static while the sensor moves. Figure 2 shows the environment at two instant of time and the motion field for some of the scan points. For clarity, the motion field has been magnified and the scanner remains static (at the position (0,0)) while the environment moves.

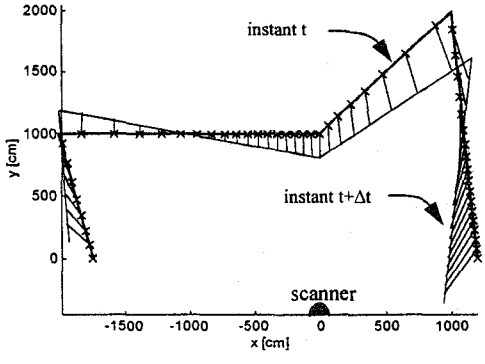

Figure 2. Velocity field due to a translation and rotation of the radial laser scanner.

The problem of recovering the motion parameters of a mobile robot can be formulated as that of matching two consecutive scans of the sequence provided by the scanner. This problem has a great importance in the mobile robot context, including pose estimation and map building. Three

This work has been supported by the Spanish Goverment under the CICYT project TAP96-0763.

different approaches have been previously proposed for doing this:

- *Feature to feature correspondence.* Registration of the two scans is accomplished by first extracting a set of features (usually segments and corners) and then making correspondences between pairs of features on the two scans. Some examples of this approach are the works presented by Shaffer et al. [8] for mobile robot pose estimation, and Gonzalez et al. [6] for map building.
- *Point to feature correspondence.* The range points of the scan are matched against features of a model or of a map obtained from previous scans. The position estimation algorithms proposed by Cox [9] and Gonzalez et al. [7] are some examples of this approach.
- *Point to point correspondence.* This scheme intends to match one range scan to another in order to derive the relative robot pose. The registration is accomplished without explicitly using the underlying features existing in the scans. A notable example is the iterative point correspondence algorithm developed by Lu [5].

The algorithm we propose falls into the latter category. It is inspired in the "optical flow constraint equation" developed by Horn and Schunck [1] for intensity images and states that the velocity of the range points is rectricted by the local structure of the environment as well as the temporal rate of change.

In the following sections we first derive the equations of the relative motion of a radial rangefinder in a rigid environment. In section 3, the equation that constraints the motion of each scanned point is presented. Next, the formulation for estimating the motion field along with the motion parameters of the sensor is proposed. In section 5, the implementation details are presented. In section 6, some experimental results with both real and synthetic data are shown. We conclude with some conclusions and future works.

2. Motion of a 2D Range Scanner in a Rigid Environment

Let V and W be the translational and rotational velocity vectors of a 2D range scanner moving on a flat surface. A point P from the environment seems to move relative to the sensor with instantaneous velocity V_P given by:

$$V_P = -W \times P - V = -\begin{bmatrix}0\\0\\w\end{bmatrix} \times \begin{bmatrix}r\cos\theta\\ r\sin\theta\\ 0\end{bmatrix} - \begin{bmatrix}u\\v\\0\end{bmatrix} \qquad (1)$$

where $[r,\theta]^T$ are the polar coordinates of the point P. Since the third component of this equation is meaningless it can be eliminated

$$V_P = -wr\begin{bmatrix}-\sin\theta\\ \cos\theta\end{bmatrix} - \begin{bmatrix}u\\v\end{bmatrix} \qquad (2)$$

On the other hand, since the velocity of the point P is the derivative of P with respect to time, we have

$$V_P = \frac{dP}{dt} = \frac{d}{dt}\begin{bmatrix}r\cos\theta\\ r\sin\theta\end{bmatrix} = \begin{bmatrix}\dot{r}\cos\theta - r\dot{\theta}\sin\theta\\ \dot{r}\sin\theta + r\dot{\theta}\cos\theta\end{bmatrix} = \qquad (3)$$

$$\begin{bmatrix}\cos\theta & -r\sin\theta\\ \sin\theta & r\cos\theta\end{bmatrix}\begin{bmatrix}\dot{r}\\ \dot{\theta}\end{bmatrix} = J\begin{bmatrix}\dot{r}\\ \dot{\theta}\end{bmatrix}$$

where J is the Jacobian of the transformation from polar to cartesian coordinates and $[\dot{r},\dot{\theta}]^T$ is the *polar velocity vector* of the point P (see figure 3).

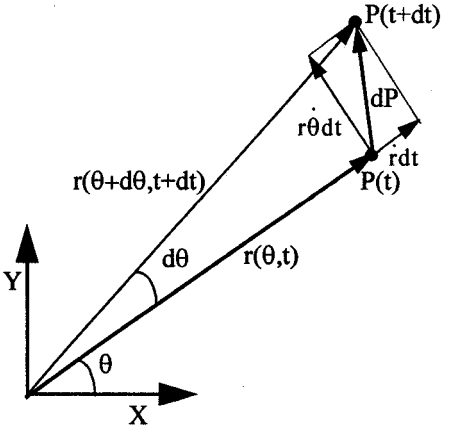

Figure 3. Motion of a point in polar coordinates.

From equations 3 and 2 it results:

$$\begin{bmatrix}\cos\theta & -r\sin\theta\\ \sin\theta & r\cos\theta\end{bmatrix}\begin{bmatrix}\dot{r}\\ \dot{\theta}\end{bmatrix} + wr\begin{bmatrix}-\sin\theta\\ \cos\theta\end{bmatrix} + \begin{bmatrix}u\\v\end{bmatrix} = 0 \qquad (4)$$

This expression holds for each point P from the scene and consists of 2 linear equations with 5 unknowns: the mobile robot motion parameters (u,v,w) and the velocity vector $[\dot{r}, \dot{\theta}]^T$. By considering the *n* points of a scan we would obtain an underconstrainted system with $2n$ equations and $2n+3$ unknowns. Consequently, some additional constraints are required to solve for the motion parameters.

Alhough neither $\dot{r}$ nor $\dot{\theta}$ can be estimated from the range scan, it is possible to establish a relationship between them by taking into account the information provided by a range scan sequence. In the following section we derive this relationship.

3. The Velocity Constraint Equation

The following formulation is inspired in the optical flow constraint equation proposed in the computer vision literature [1].

Let $r(\theta,t)$ be the range measured for a generic point P at scan angle θ and time t. At a some later time t+dt the point P will be scanned at a angle $\theta+d\theta$ with the range:

$$r(\theta + d\theta, t + dt) = r(\theta, t) + \frac{\partial r}{\partial \theta} d\theta + \frac{\partial r}{\partial t} dt + O(e) \qquad (5)$$

where $O(e)$[1] denotes the higher order terms in $d\theta$ and dt.

Subtracting $r(\theta,t)$ from both sides of equation 5, neglecting O(e), dividing through by "dt" and taking the limit dt—>0 we obtain

$$\dot{r} = \frac{d}{dt} r(\theta, t) = \frac{\partial r}{\partial \theta}\frac{d\theta}{dt} + \frac{\partial r}{\partial t} = r_\theta \dot{\theta} + r_t \qquad (6)$$

where r_θ and r_t are the partial derivatives of the range function with respect to the angle θ and time t, respectively, which can be estimated from the range scan sequence.

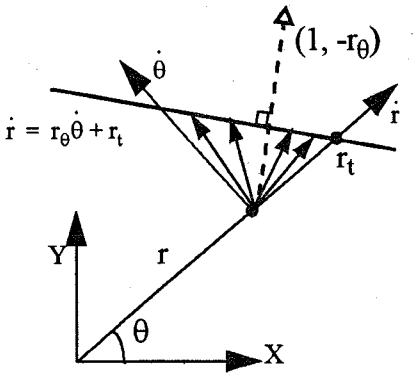

Figure 4. A visual interpretation of the *velocity constraint equation.*

Equation 6 states a constraint over the possible velocities that a point from the scene can reach once the local structure of the environment (r_θ) and the temporal rate of change (r_t) have been estimated for a given range point $[r,\theta]^T$. We call this equation the *velocity constraint equation.* To illustrate it graphically, consider the polar velocity space ($\dot{r}$-$\dot{\theta}$) where equation 6 represents a line with slope r_θ and ordinate at the origin r_t (see figure 4).

Assuming that r_θ and r_t are known at a given instant of time t and angle θ, the polar velocity vector of the scanned point at θ can not be an arbitrary one: its component in the direction $[1,-r_\theta]^T$ (perpendicular to the surface) is

$$\frac{-r_t}{(1 + r_\theta^2)^{1/2}}$$

However, the component of the velocity vector in the direction tangent to the object can not be determined. Notice the analogy with the *aperture problem* reported by Horn and Schunck [1] for the case of the optical flow.

4. Estimating the Motion Parameters and Solving for the Motion Field

The formulation we derive here is somehow similar to the one reported by Horn and Negahdaripour for direct passive navigation [2]. In our case, however, it is not necessary to incorporate into the formulation physical constraints like planar or quadratic surfaces.

According to equation 6, the polar velocity vector has only one degree of freedom, for example $\dot{\theta}$, and can be expressed as:

$$\begin{bmatrix} \dot{r} \\ \dot{\theta} \end{bmatrix} = \begin{bmatrix} r_\theta \dot{\theta} + r_t \\ \dot{\theta} \end{bmatrix} = \begin{bmatrix} r_\theta \\ 1 \end{bmatrix} \dot{\theta} + \begin{bmatrix} r_t \\ 0 \end{bmatrix} = R_\theta \dot{\theta} + R_t \qquad (7)$$

Using the velocity constraint equation derived above along with equation 4, we obtain the following two linear equations for the unknowns $\dot{\theta}$,w,u,v:

$$JR_\theta \dot{\theta} + JR_t + wr \begin{bmatrix} -\sin\theta \\ \cos\theta \end{bmatrix} + \begin{bmatrix} u \\ v \end{bmatrix} = 0 \qquad (8)$$

This equation has still two degrees of freedom. Since each scanned point provides two additional constraints (equations) and only one additional unknown (its angular velocity $\dot{\theta}$), a minimum of three scanned points will suffice to solve for the six unknowns ($\dot{\theta}_1$, $\dot{\theta}_2$, $\dot{\theta}_3$,w,u,v).

In practice, the solution obtained by using the minimum number of points (i.e. equations) is noisy because of noise in the range scans, quantization errors, and errors in estimate derivatives using finite difference methods. By considering *n* scanned points, the total number of equations becomes 2*n* while the number of unknowns is *n*+3. It leads to a least-squares formulation that allows to recover more robustly and accurately the robot motion parameters. This formulation will be derived in detail in the next section.

5. Implementation

To use the proposed formulation with a range scan se-

1.- We are assuming the angular and temporal smoothness of the function $r(\theta,t)$.

quence we need to formulate equation 8 in a discrete fashion as well as to combine in a matrix form all the equations provided by the points being considered.

Let r_k be the range at the discrete angle θ_k. Using the subscript "k" to denote the fact that the functions are evaluated at the discrete angle θ_k, equation 8 can be rewritten:

$$J_k(R_\theta)_k\dot{\theta}_k + J_k(R_t)_k + wr_k\begin{bmatrix}-\sin\theta_k\\ \cos\theta_k\end{bmatrix} + \begin{bmatrix}u\\ v\end{bmatrix} = 0 \qquad (9)$$

where the partial derivatives $(r_\theta)_k$ and $(r_t)_k$ in $(R_\theta)_k$ and $(R_t)_k$ respectively, can be estimated from the range scan sequence using numerical differentiations [3]:

$$(r_\theta)_k = \frac{r_{k+1}(t) - r_{k-1}(t)}{2\Delta\theta}$$

$$(r_t)_k = \frac{r_k(t) - r_k(t-\Delta t)}{\Delta t}$$

with Δt being the time between consecutive scans. As a 2D laser range sensor scans radially at a fixed angular increment we have

$$\Delta\theta = \theta_k - \theta_{k-1} = \text{constant} \qquad \forall k$$

Equation 9 can be rewritten more conveniently in the form

$$\begin{bmatrix}J_k(R_\theta)_k & I & Q_k\end{bmatrix}\begin{bmatrix}\dot{\theta}_k\\ u\\ v\\ w\end{bmatrix} = -J_k(R_t)_k \qquad (10)$$

where I is the 2x2 identity matrix and $Q_k=[-r_k\sin\theta_k\ r_k\cos\theta_k]^T$.

Let $\{r_k, k=1,\ldots,n\}$ be a range image taking at time t. Since each range r_k gives rise to a pair of equations 10 we obtain the following system of $2n$ linear equations and n+3 unknowns:

$$\begin{bmatrix}J_1(R_\theta)_1 & 0 & \ldots & 0 & I & Q_1\\ 0 & J_2(R_\theta)_2 & \ldots & 0 & I & Q_2\\ \ldots & \ldots & \ldots & \ldots & \ldots & \ldots\\ 0 & 0 & \ldots & J_n(R_\theta)_n & I & Q_n\end{bmatrix}\begin{bmatrix}\dot{\theta}_1\\ \dot{\theta}_2\\ \ldots\\ \dot{\theta}_n\\ u\\ v\\ w\end{bmatrix} = -\begin{bmatrix}J_1(R_t)_1\\ J_2(R_t)_2\\ \ldots\\ J_n(R_t)_n\end{bmatrix} \qquad (11)$$

Since the system is overconstrainted we define an error vector E with $2n$ components

$$E = AX - B \qquad (12)$$

where A is the $2nxn$+3 matrix on the left side of equation 11, X is the unknown vector and B is the vector on the right.

The least-squares solution of equation 12 is

$$X = (A^TA)^{-1}A^TB$$

Notice that the number of points n in a scan may be up to several hundreds or even thousands, what makes computationally prohibited to invert the matrix A^TA, which dimension is n+3xn+3. Fortunately, it is a really special matrix that beside to be symmetric it is mostly diagonal, as shown in figure 5. Thus, to find the inverse of matrix A^TA we can decompose it as follows [4]:

$$(A^TA)^{-1} = \begin{bmatrix}M & N\\ O & P\end{bmatrix}^{-1} =$$

$$\begin{bmatrix}M^{-1}+M^{-1}N(P-OM^{-1}N)^{-1}OM^{-1} & -M^{-1}N(P-OM^{-1}N)^{-1}\\ -(P-OM^{-1}N)^{-1}OM^{-1} & (P-OM^{-1}N)^{-1}\end{bmatrix}$$

provided $|M| \neq 0$ and $|P-OM^{-1}N| \neq 0$, where M is an nxn diagonal matrix and N, O and P are matrices of dimensions nx3, 3xn and 3x3, respectively. As A^TA is a symmetric matrix, P has to be symmetric and O has to be equal P. This reduces significantly the computational burden.

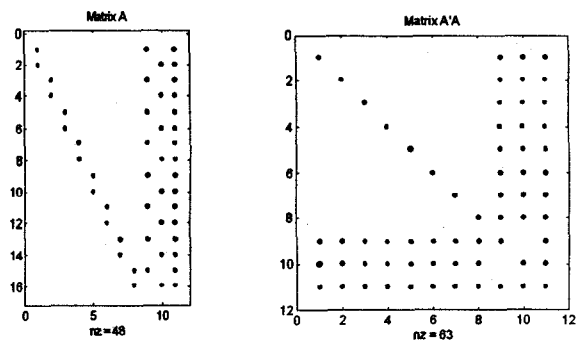

Figure 5. Nonzero (nz) elements of the matrices A and A^TA for n=8 (see text).

6. Some Experiments

In this section some results are presented to demonstrate the performance of the proposed method. Most of the tests have been carried out using synthetic data since the motion of the scanner can exactly be known. In particular, the results shown in this section are obtained from the scenario shown in figure 6. Another kind of scenario has provided similar results, except in some degenerated cases like an infinite wall or a long corridor where one of the motion components becomes undetermined.

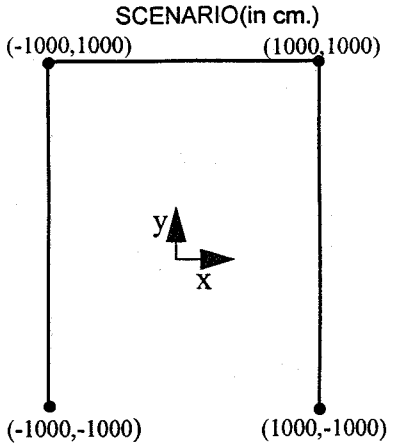

Figure 6. Synthetic scenario used for the simulated tests.

In the simulated experiments we construct the sequence by scanning at fixed translational and rotational intervals (named "stepx", "stepy" and "stepang", respectively). At each of the positions, the translational and rotational components of the displacement are computed by the proposed algorithm and the corresponding error (true minus computed) is recorded.

Following we include some plots showing the errors obtained when using different number of range points (figure 7) and different displacement between consecutive scans (figure 8). The errors shown are expressed relative to the true displacement (i.e. error divided by the true displacement) while the abcissas axis represents the different steps along the sequence.

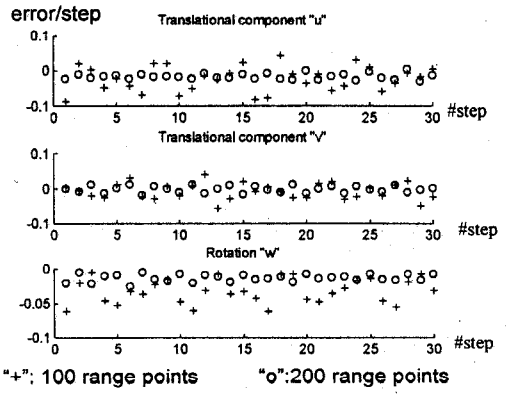

Figure 7. Motion errors for two different number of range points. The true displacement was stepx=4cm. stepy=4cm. and stepang=0.01rad.

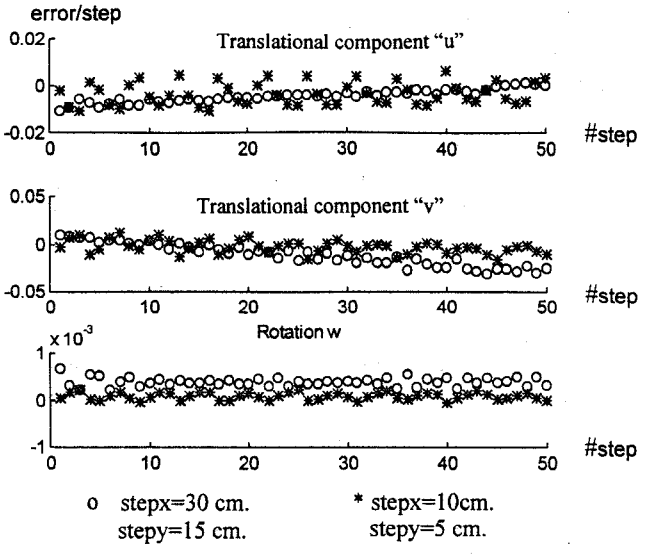

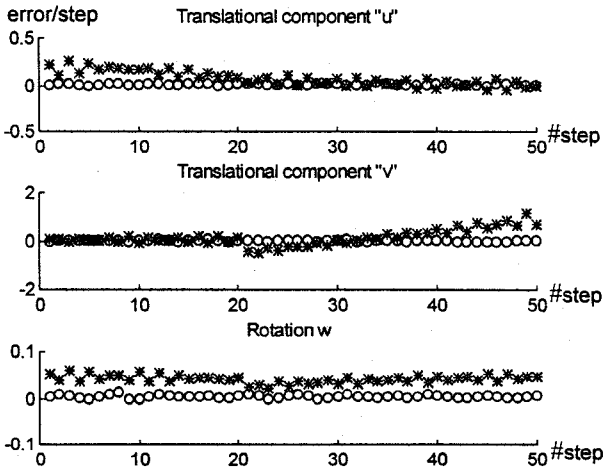

FIGURE 8. Errors in the displacement for a pure translation with two different translational parameters (above), and for two different rotational parameters and a translation of stepx=5cm., stepy=2cm. (below). In both experiments the number of range points is 200.

As expected, the bigger the number of scanned points and the smaller the displacement the better the results, that is, the error in the estimate motion depends on how close the discrete formulation is from the continuos case. From the above and other conducted experiments we have also tested that smooth surfaces yield better results than irregular ones. We have observed that discontinuities in the contour produce significant errors since the higher order term in equation 5 are not negletable. This is an aspect in which currently we are working on.

The proposed algorithm has also been tested using real data provided by a laser rangefinder called "PLS", manufactured in Germany by Sick Optic-electronic Inc. This sensor has a range resolution of 5cm, an accuracy of

±20cm, and provides up to 360 measures in a 180 degrees field of view. The experiment consists of taking 10 stationary scans at known positions equally separated 5cm. with no rotation. Figure 9a shows the scans taken at the first and last position from the sequence. Figure 9b plots the errors for the 9 displacements. Notice that, in this case the error plotted is not percentual but true displacement minus computed displacement.

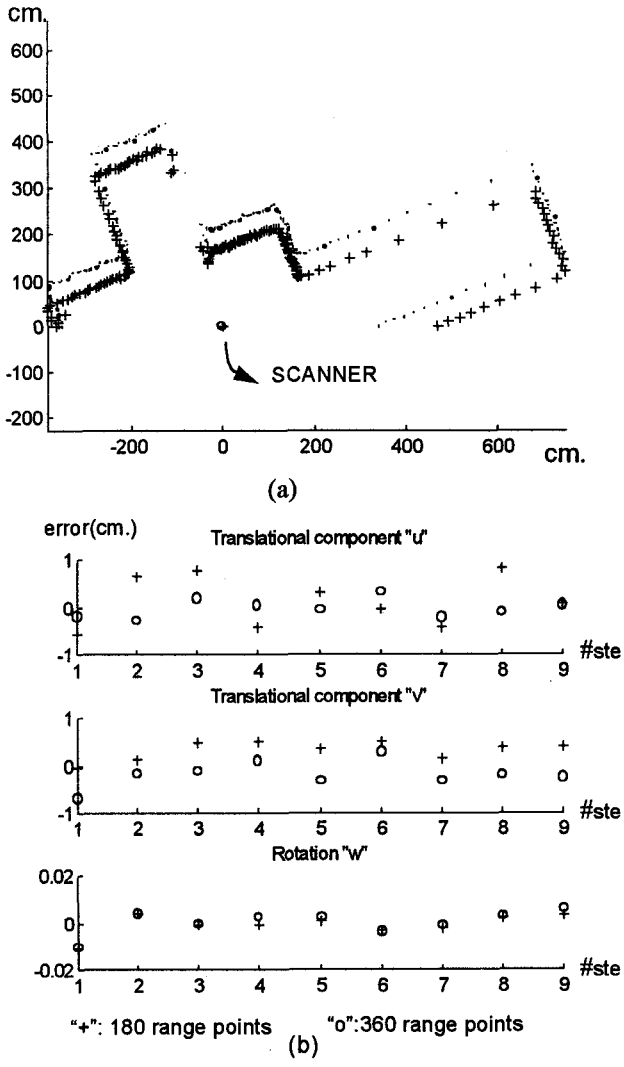

Figure 9. (a)Scans taken at the first and last position. (b) Errors obtained for the 9 displacement (stepx=5cm., stepy=0 cm., stepang=0 degrees)

7. Conclusions and Future Works

In this paper we have presented a new approach to recover the instantaneous motion of a radial laser rangefinder along with the motion field of the range points in the scans.

It has been presented experimental results showing that good results are achieved with both real and synthetic data. Although we have concentrated in estimating the motion parameters of the mobile robot, we think that the motion field can be very useful for a number of applications, including range image segmentation and object motion detection and tracking.

Currently we are trying to improve the performance of the proposed algorithm by tackling some problems that have emerged from this preliminary work. These problems include: noise reduction, integration of different scans by using, for example, a Kalman Filter, and automatically discarding those range points that strongly violates the velocity constraint equation. We also plan to extend this formulation to 3D laser scanners.

References

[1] B.K.P Horn and B.G. Schunck. "Determining Optical Flow" Artificial Intelligence. vol 17, pp. 185-203. 1981.

[2] B.K.P. Horn and S. Negahdaripour. "Direct Passive Navigation: Analytical Solution for Planes". IEEE Trans. Pattern Analisys and Machine Intelligence 9 (1)168-176. 1987.

[3] J.H. Mathew. "Numerical Methods for Mathematics, Science and Engineering" (Second Edition). Prentice Hall International. 1992.

[4] K. Ogata. "Modern Control Engineering" (Second Edition). Prentice Hall International. 1990.

[5] F. Lu. "Shape Registration using Optimization for Mobile Robot Navigation". PhD. Dissertation. Univ. of Toronto. Canada. 1995.

[6] J. Gonzalez, A. Ollero and A. Reina. " Map Building for a Mobile Robot equipped with a Laser Range Scanner". *IEEE Int. Conference on Robotics and Automation*, San Diego, CA, USA, May 1994.

[7] J. Gonzalez, A. Stentz and A. Ollero."A Mobile Robot Iconic Position Estimator using a Radial Laser Scanner". *Journal of Intelligent&Robotic Systems 13:161-179. Kluwer Academic Press.* 1995.

[8] G. Shaffer, A. Stentz, W. Whittaker, K. Fitzpatrick. "Position Estimator for Underground Mine Equipment". In *Proc. 10th WVU International Mining Electrotechnology Conference*, Morgantown, W. VA, July 1990.

[9] I. C. Cox. "Blanche-An Experiment in Guidance and Navigation of an Autonomous Robot Vehicle". IEEE Transactions on Robotics and Automation, Vol. 7, no. 2, April 1991.